Magnetic neutron scattering study of single-crystal cupric oxide

B. X. Yang
Department of Physics, University of British Columbia, Vancouver, British Columbia, Canada V6T 2A6

T. R. Thurston
Department of Physics, Massachusetts Institute of Technology, Cambridge, Massachusetts 02139

J. M. Tranquada and G. Shirane
Physics Department, Brookhaven National Laboratory, Upton, New York 11973
(Received 24 October 1988)

Among Cu^{2+} compounds, cupric oxide (CuO) has unusual magnetic properties, some of which are shared by the superconducting copper oxides. In order to study these properties further, neutron scattering experiments on a CuO single crystal have been performed. Two magnetic phase transitions at $T_{N1}=231$ K and $T_{N2}=212.5$ K have been observed, with the magnetic structure below T_{N2} antiferromagnetic and the structure between T_{N1} and T_{N2} helical in nature. The dynamics of the magnetism was also studied. As in La_2CuO_4, the dispersion of the low-temperature spin-wave excitations is unusually steep ($dE/dk=250\pm75$ meV Å^{-1}), indicating strong magnetic interactions. Inelastic magnetic scattering has also been measured above T_{N1}. At temperatures slightly above the 231-K phase transition, dynamic critical slowing has been observed.

INTRODUCTION

Magnetic materials containing the Cu^{2+} ion play an important role in the study of magnetism. The ion has a $3d$ hole whose orbital moment is often completely quenched in crystalline environments, and, consequently, it behaves like an isotropic "spin-only" system ($S=\frac{1}{2}$). It is often found in antiferromagnetic Heisenberg systems, especially those of one or two dimensions.[1] Typical g values, as measured by many techniques, are close to 2. In many of these systems, the magnetic interaction between the Cu^{2+} ions is enhanced in one or two directions through superexchange due to the intervening anions. Cupric oxide (CuO), however, shows many distinct magnetic properties from other Cu^{2+} compounds, as well as from other $3d$ transition-metal magnetic monoxides. It has been discovered recently that some of these interesting magnetic properties are shared by the new superconducting copper oxides.

The discovery of antiferromagnetism in La_2CuO_4 (Refs. 2–4) and $YBa_2Cu_3O_7$ (Ref. 5) has encouraged speculation that magnetic interactions are important for hole pairing in these new superconductors. The report[6] of strong two-dimensional magnetic correlations within the CuO_2 planes in La_2CuO_4 at temperatures well above the Néel temperature has generated further excitement. Studies of similar magnetic systems should allow one to identify those features which are unique to the layered cuprates. We have, therefore, undertaken a study of the structure and dynamics of the spin system in CuO, a system which consists of strongly interacting Cu^{2+} ions, but which does not have two-dimensional CuO_2 planes.

Cupric oxide occurs in nature as paper-thin twinned aggregates (tenorite). It is a steel-grey-to-black stoichiometric semiconductor. An antiferromagnetic phase transition at about 220 K was first indicated by specific-heat measurements,[7,8] and later confirmed by a neutron-diffraction experiment.[9] This transition temperature is much higher than in most previously studied Cu^{2+}-based magnetic systems, whose transition temperatures are typically in the range of a few degrees kelvin. In addition, the magnetic susceptibility[10,11] of CuO showed another interesting phenomenon: The susceptibility continues to rise above the Néel temperature and does not reach its maximum until 540 K. Since such behavior is not uncommon in Heisenberg systems with strong one-dimensional character,[1] a reasonable speculation is that CuO behaves like a one-dimensional antiferromagnet above the three-dimensional phase transition temperature. However, O'Keefe and Stone,[10] making an analogy with cupric acetate whose susceptibility showed a similar broad maximum, used a molecular antiferromagnetism (noncooperative) model to interpret their data. The broad maximum in susceptibility was attributed to thermal excitation of the first excited state of a pair of copper atoms. The energy of the first excited (triplet) state, and thus the strength of the exchange interaction, were derived from the experimental data to be $J=90.5$ meV.

The crystal structure (Fig. 1 and Table I) of CuO has been studied by x-ray diffraction.[12–14] Unlike the usual rocksalt structure of other $3d$ transition-metal monoxides, the structure of CuO is monoclinic with $C2/c$ symmetry and with four formula units per unit cell. The copper ions occupy symmetry site $4(c)$, $(x,y,z)=(\frac{1}{4},\frac{1}{4},0)$, and the oxygen ions take position $4(e)$, $(x,y,z)=(0,y,\frac{1}{4})$ with $y=0.416(2)$. The strength of the superexchange interaction between Cu atoms depends on the Cu–O–Cu bond angle and should be strongest for angles near 180°. The structure of CuO can be viewed as consisting of chains along the $[10\bar{1}]$ direction in which the Cu–O–Cu angle is[14] 146°; Cu–O–Cu bond angles in other directions are all less than 109°. One therefore expects that the strong-

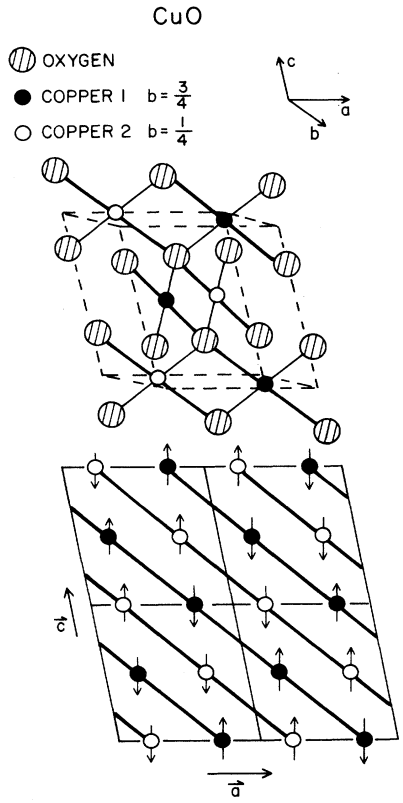

FIG. 1. (a) The crystal structure of cupric oxide. (b) Positions of copper ions projected on the (010) plane.

est superexchange should occur within the $[10\bar{1}]$ chains. The first neutron-diffraction study of CuO by Brockhouse[9] reported a periodic arrangement of the magnetic moments and also set the lower limit for the ordered moment at $0.5\mu_B$ per Cu ion. In an attempt to better characterize this system, Yang, Tranquada, and Shirane[15] reexamined these early measurements by conducting a more detailed powder diffraction experiment. They confirmed the antiferromagnetic ordering below 225 K by polarized neutron diffraction, and determined that the magnetic unit cell has a volume double that of the chemical unit cell, with spin directions alternating along the $[10\bar{1}]$ chains (Fig. 1). The ordered moment was found to be $0.68\mu_B$ per Cu, significantly smaller than the $1\mu_B$ expected for a spin-only Cu^{2+} ion. They also noticed a broad peak around the $(\frac{1}{2}0\frac{\bar{1}}{2})$ position above T_N, suggesting that strong one-dimensional correlations may exist at high temperatures. In this paper, we investigate further the magnetic scattering in CuO in a single-crystal experiment.

TABLE I. Lattice constants of CuO (monoclinic, $C2/c$, space group No. 15).

Source	a (Å)	b (Å)	c (Å)	β	y
a	4.662	3.417	5.118	99.48°	0.416
b	4.684	3.425	5.129	99.28°	
c	4.6837	3.4226	5.1288	99.54°	0.4184
d	4.6837	3.4226	5.1288	99.54°	0.4162
e	4.631		5.069	99.60°	

[a] Reference 12 (at room temperature).
[b] Reference 13 (26 °C).
[c] Reference 14 (at room temperature).
[d] Reference 15 ($T=300$ K).
[e] This work. The constants b and y are not available from the diffraction data in the $(H0L)$ zone.

CRYSTALLINE AND MAGNETIC STRUCTURE

The crystal used in this experiment was grown by Atomergic Chemicals, Inc., New York. Its dimensions were $10\times3\times0.5$ mm^3, and it was of shiny black appearance. The mosaic of the crystal was about 1°, with a non-Gaussian spread. In all experiments reported here, the crystal was mounted on the cold finger of a liquid-nitrogen flow cryostat. The b axis was chosen to be perpendicular to the scattering plane, i.e., the experiment was carried out in the $(H0L)$ zone.

Neutron scattering measurements were made on spectrometers H4M and H9 at the Brookhaven High Flux Beam Reactor. A pyrolytic graphite (PG) (002) reflection was used to both monochromatize and analyze the neutron beam, and PG filters were used to suppress second-order neutrons. A variety of different neutron energies and spectrometer collimation configurations were used for the different measurements reported here.

The lattice constants of this crystal at room temperature are listed in Table I. One should note that a and c are less than all previously measured values by about 1%. Since the crystal has not been annealed in oxygen after growth, its oxygen concentration is expected to be lower than previously studied samples. Thus, the difference in lattice constants is most likely due to variations in oxygen concentration.

At $T_{N1}=231\pm2$ K, two magnetic peaks develop at $(\frac{1}{2}0\frac{\bar{1}}{2})\pm\tau$, where $\tau=(0.0125,0,0.0125)$. This temperature is in rough agreement with, but somewhat higher than the Néel temperature obtained previously by specific-heat measurements,[10,11] magnetic-susceptibility measurements,[8] and neutron-diffraction measurements from powder samples.[9] As the temperature is lowered further, the position of the two magnetic peaks remains unchanged, but their intensity increases until a second phase transition occurs at $T_{N2}=212.5\pm1.0$ K (on cooling). At this temperature, the two magnetic peaks abruptly disappear, and a strong single peak develops at the $(\frac{1}{2}0\frac{\bar{1}}{2})$ position. In the following, we shall refer to the magnetic structure between T_{N1} and T_{N2} as the intermediate phase, and the magnetic structure below T_{N2} as the low-temperature phase.

The magnetic structure of the low-temperature phase was determined previously by powder neutron diffraction as discussed in the Introduction. The spin structure is shown in Fig. 1; the spin direction is along the b axis. Integrated Bragg intensities have been measured on the sin-

gle crystal at 150 K for eight magnetic and five nuclear reflections. To compare the present measurements with the earlier work, we used the known spin structure to extract the magnetic form factor $f(\mathbf{Q})$ for Cu from the integrated intensities. The results are shown in Fig. 2, where they are compared with the spherically symmetric, spin-only form factor calculated[16] for Cu^{2+}. The experimental values have been normalized so that the value corresponding to the $(\frac{1}{2}0\frac{\bar{1}}{2})$ value matches the calculation. The differences between the measured and calculated form factors, which are probably due to nonspherical components of the spin density, are of reasonable magnitude, and the overall agreement indicates that the spin structure is basically correct. Scaling the magnetic intensities to the nuclear ones and taking the form-factor normalization into account, we obtain an effective moment of $0.69 \pm 0.05 \mu_B$ per Cu atom.

Figure 3 shows transverse scans around the strongest magnetic peak, the $(\frac{1}{2}0\frac{\bar{1}}{2})$, at temperatures around T_{N1} and T_{N2}. The intermediate phase is characterized by the splitting of the magnetic peaks at the $(h/2\,0\,l/2)$ positions [h,l odd, and $(h+l)/2$=even number], indicating that while the spin arrangement is still Néel-like in the $[10\bar{1}]$ chains, it also has a long period (80 lattice constants) superstructure along the [101] direction. We also found that the relative intensities of the two intermediate phase peaks varies randomly as the temperature is cycled through T_{N1}. Behavior similar to this has been observed in Rb_2MnF_4,[17] where it occurs because two magnetic structures have comparable free energies.

For an antiferromagnet in the Néel state, the magnetic peak intensity is proportional to the square of the sublattice magnetization. By integrating the magnetic peak intensity in scans such as those in Fig. 3, we obtained the magnetization curve shown in Fig. 4. In the temperature range between T_{N1} and T_{N2}, the values shown are the sums of the two magnetic peaks from the intermediate structure. While the magnetization changes gradually with temperature near T_{N1}, indicating a second-order

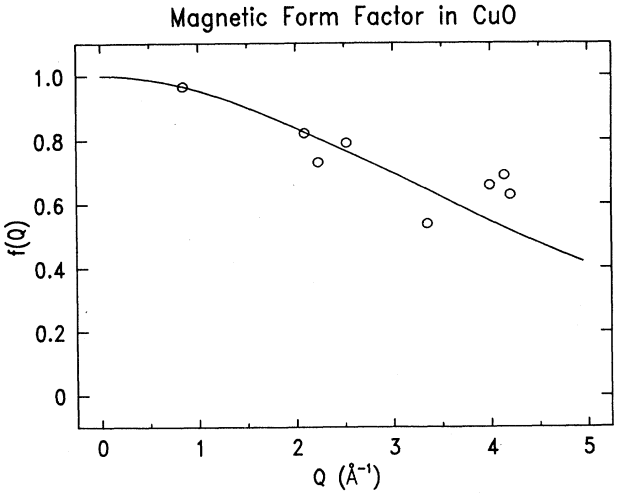

FIG. 2. Observed (circle) and calculated (line) values of $f(\mathbf{Q})$, as discussed in the text.

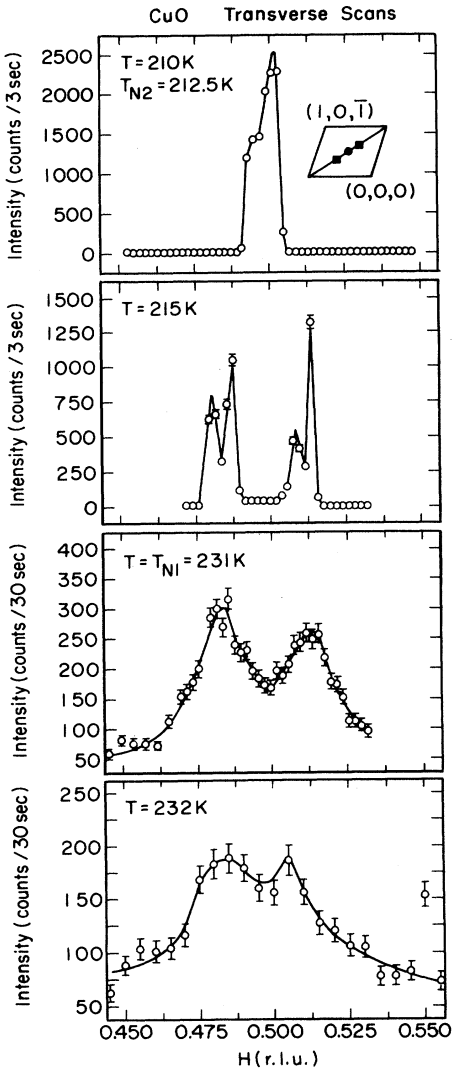

FIG. 3. Transverse scans through $(\frac{1}{2}0\frac{\bar{1}}{2})$. The critical scattering can be seen clearly in the scans a few degrees above T_{N1}. Below T_{N1}, the spins first form an intermediate structure with a long-period superstructure in the [101] direction; the structure then transforms to a complete Néel state below T_{N2}. The top two scans show the Bragg peaks associated with these two phases.

phase transition, the transition near T_{N2} is abrupt and shows hysteresis, indicating a first-order transition. In Fig. 4, we also show the specific-heat data of Millar,[7] and Hu and Johnston.[8] The two transitions observed in this experiment correlate well with the two specific-heat anomalies observed by Millar.[7] Furthermore, the nonreproducible feature around T_{N2} discussed by Millar can be correlated with the hysteresis observed around T_{N2}. Since no attempt was made to determine the oxygen content in the samples used in both specific-heat experiments, it is not inconceivable that the inconsistency between the two measurements is due to different oxygen concentrations in their samples.

Figure 5 shows the scattering intensity at the $(\frac{1}{2}0\frac{\bar{1}}{2})$

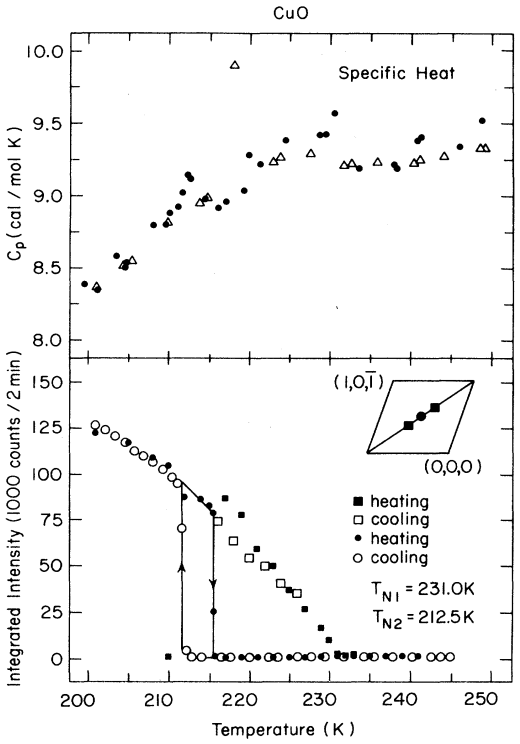

FIG. 4. (a) Specific heat of CuO vs temperature. The data of Millar (Ref. 7) show two transitions at T_{N1} and T_{N2}, while those of Hu and Johnson (Ref. 8) show only one transition but a larger specific anomaly. The discrepancy may be due to different oxygen contents in the samples studied in the experiments. (b) Integrated intensities of the magnetic peaks at and in the vicinity of $(\frac{1}{2}\,0\,\bar{\frac{1}{2}})$ as a function of temperature. The intensities between T_{N1} and T_{N2} are the sums of two magnetic peaks. Hysteresis around T_{N2} can be seen in these measurements.

position as a function of temperature. A typical pattern of critical scattering can be clearly seen around T_{N1}, where the intensity of a position on the tails of an incipient Bragg peak reaches a maximum at the transition temperature due to critical fluctuations. Scans were performed above T_{N1} in both longitudinal and transverse directions. The longitudinal scans were subsequently fitted to a Lorentzian convolved with the measured Gaussian resolution function, and the transverse scans to two Lorentzians convolved with the measured Gaussian resolution function. The inverse correlation length κ for the longitudinal and transverse directions extracted from these fits is shown in Fig. 5 (inset). Although the correlation lengths are clearly anisotropic, both the longitudinal and transverse values are increasing and of similar magnitude as the temperature approaches T_{N1}. The transition at T_{N1} is therefore three dimensional in nature.

INELASTIC NEUTRON SCATTERING

Detailed inelastic neutron scattering experiments were performed at 150 and 250 K on spectrometer H4M. In all of these experiments, the energy of the scattered neutrons was held fixed at 14.7 meV, and the energy transfer was varied by our changing the incident neutron energy. The normalization of the scattered beam intensity to the incident flux has been corrected for the presence of higher-order neutrons in the incident beam.[18]

Experiments at 150 K were performed to characterize the low-energy excitations and to measure the spin-wave velocity v. A scan of energy transfer with the momentum transfer held fixed at the $(\frac{1}{2}\,0\,\bar{\frac{1}{2}})$ position is shown in Fig. 6. Peaks are seen on each side of the elastic (Bragg) peak, indicating long-wavelength spin excitations of finite energy. The spin-wave energy gap, excitation energy for the $\mathbf{Q}=\mathbf{0}$ mode, is 2.5 ± 0.5 meV.

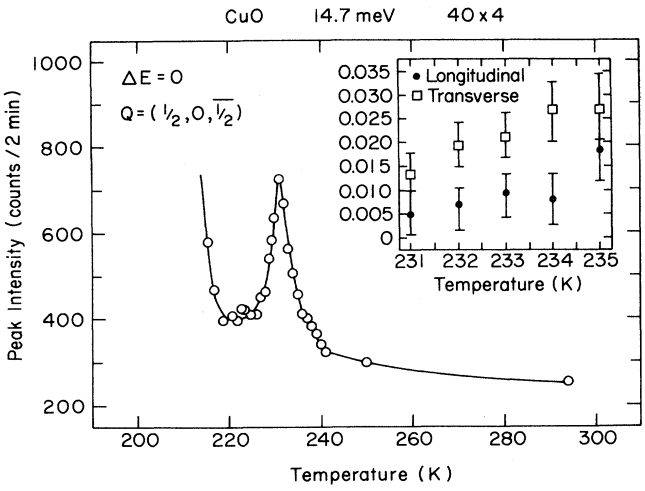

FIG. 5. Critical scattering at $(\frac{1}{2}\,0\,\bar{\frac{1}{2}})$ near the magnetic transitions. Inset: Temperature dependence of the inverse correlation length κ in the longitudinal [10$\bar{1}$] and transverse [101] directions.

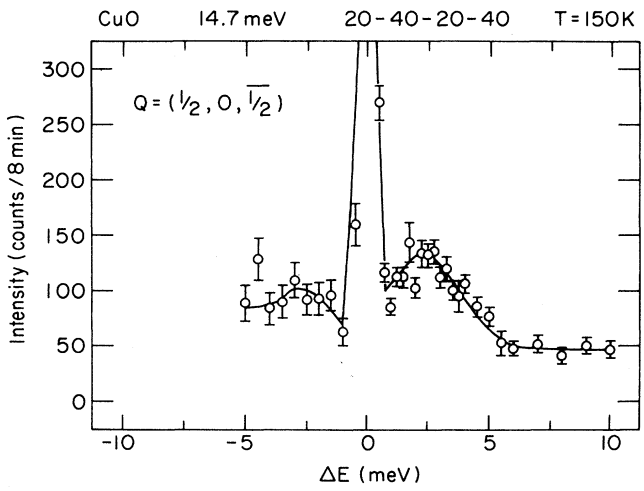

FIG. 6. $T=150$ K energy scan at the $(\frac{1}{2}\,0\,\bar{\frac{1}{2}})$ magnetic Bragg peak. The two side peaks are from spin-wave scattering, and the central peak is Bragg scattering. The line is a fit to Eq. (1) plus a Gaussian.

A series of scans in which the energy transfer was held fixed while the momentum transfer was scanned longitudinally through the $(\frac{1}{2}0\frac{\bar{1}}{2})$ peak is shown in Fig. 7(a). The spectrometer collimation used in these scans was 40-40-40-40, which gave an energy resolution of 1.0 to 1.4 meV full width at half maximim (FWHM) depending on the energy transfer. A fit to a simple Heisenberg antiferromagnetic cross section[19]

$$S(\mathbf{Q},\omega)=\left(\frac{1}{1-e^{-\beta E}}\right)\left(\frac{\Gamma}{\Gamma^2+(E-E_{\mathbf{Q}})^2}+\frac{\Gamma}{\Gamma^2+(E+E_{\mathbf{Q}})^2}\right)\frac{1}{E}, \quad (1)$$

convolved with the experimental resolution function is also shown. In this cross section, the spin-wave energy $E_{\mathbf{Q}}$ was set equal to $[E_{\text{gap}}^2+v^2(Q_h^2+Q_k^2+Q_l^2)]^{1/2}$. We are aware of the fact that the excitations are not isotropic in the reciprocal space, but our data do not warrant a more detailed analysis. Figure 7(b) shows the resolution function relative to the spin-wave dispersion. Clearly, with this spectrometer configuration, the energy-momentum resolution does not allow us to determine the intrinsic width of the spin-wave peaks. Hence, the spin-wave lifetime, Γ, was set equal to a value much smaller than resolution, 0.5 meV, in the fit. The fit to the data gave the spin-wave velocity $v=250\pm75$ meV Å. From this measurement a rough estimate of J may be found by our using the results of spin-wave theory for a quasi-one-dimensional Heisenberg antiferromagnet. In that case the velocity is equal to Ja, where a is the nearest-neighbor spacing. If we take $a=3.75$ Å, the Cu-Cu distance along the $[10\bar{1}]$ direction, then $J\simeq67\pm20$ meV. This value is of the same magnitude as the exchange constant in La_2CuO_4 (115 meV),[6,20] while it is much greater than the exchange in most previously studied ionic antiferromagnets,[21] where typical values are less than 10 meV.

Longitudinal scans through $(\frac{1}{2}0\frac{\bar{1}}{2})$ with fixed energy transfer were also performed above T_N at 250 K (see Fig. 8). Although there is some broadening of the peaks, the scattering intensity at each energy (except $\Delta E=0$) is quite similar to that observed at 150 K. The relatively narrow peak widths indicate that the magnetic correlation length is still fairly large. We have also observed a weaker, broadened peak at 290 K and an energy transfer of 4 meV. The strong correlations above T_N are consistent with the large exchange constant.

In order to test whether CuO exhibits classical critical slowing as the temperature is lowered through T_{N1}, a series of inelastic scans were performed on spectrometer H9. The spectrometer configuration used was 60-40-60-80-80 with $E_f=4.0$ meV; in this configuration the energy resolution is 0.08 meV. Figure 9 shows a scan at $T=232$ K with the momentum transfer set at $q=0.023$ Å^{-1} away from the intermediate phase peak position in the transverse direction. The incoherent background has been removed, and the line corresponds to a fit of a Lorentzian convolved with a Gaussian resolution function. The energy width obtained from this fit is 0.35 meV; furthermore, a scan at $T=231$ K gave a width of 0.25 meV. From this

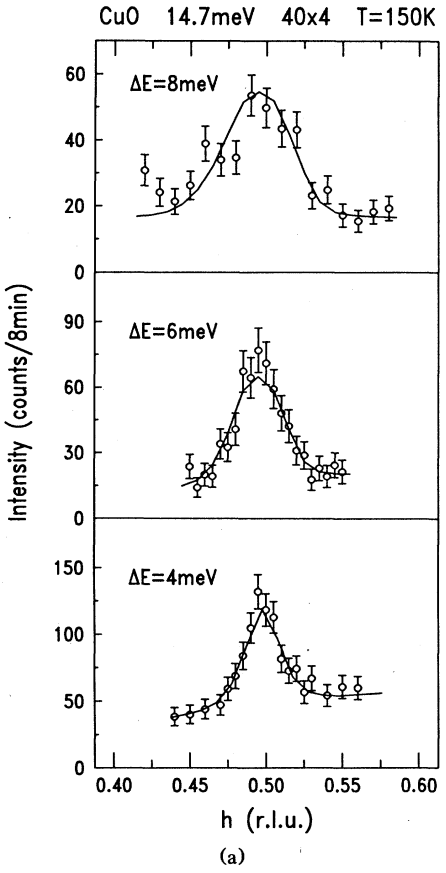

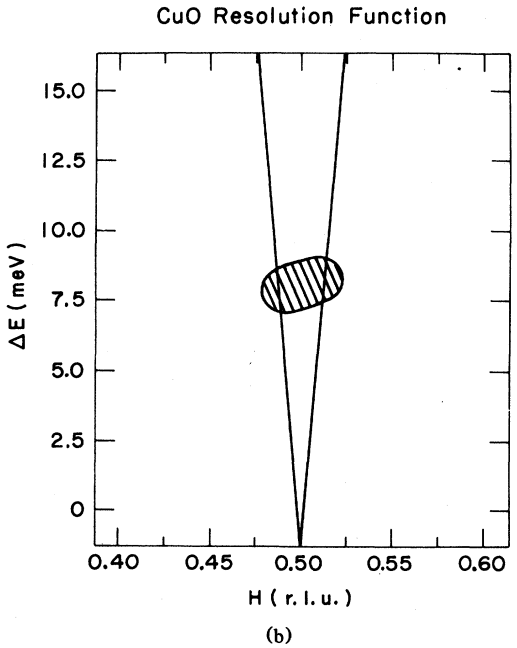

FIG. 7. (a) Constant energy longitudinal scans through the $(\frac{1}{2}0\frac{\bar{1}}{2})$ magnetic Bragg peak at 150 K. The lines are fits to Eq. (2) plus a sloping background. (b) Calculated resolution function at $\Delta E=8$ meV. The dispersion of the spin waves shown here is 250 meV Å.

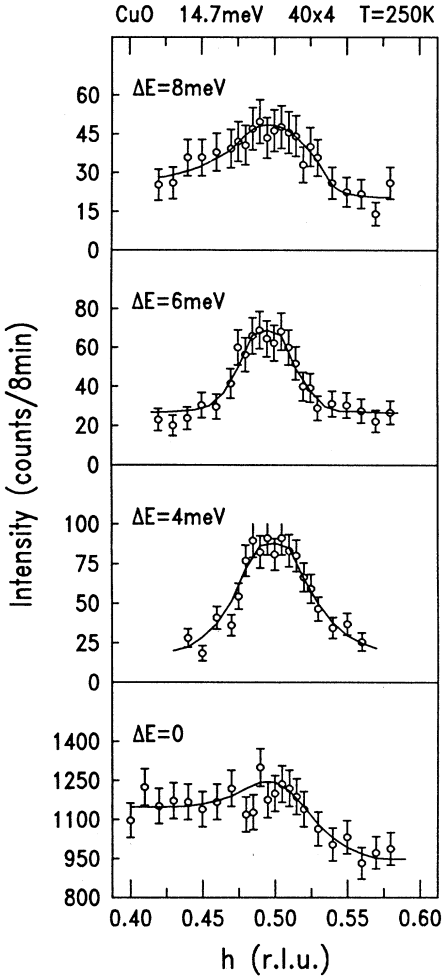

FIG. 8. Constant energy longitudinal scans through the $(\frac{1}{2}0\frac{1}{2})$ peak position at 250 K. The lines are guides to the eye.

result we conclude that the dynamic critical slowing found in other antiferromagnets is also present in CuO.

DISCUSSION

After this work was essentially completed, we became aware of the single-crystal neutron-diffraction study by Forsyth, Brown, and Wanklin.[22] They have observed the same two magnetic phase transitions reported here. In the commensurate phase they have measured a larger number of reflections and have analyzed the nonspherical components of the Cu spin density. They obtain a low-temperature copper moment of $0.65 \pm 0.03 \mu_B$, in good agreement with the value of $0.69 \pm 0.05 \mu_B$ obtained here. In the intermediate phase they observe the incommensurate peaks displaced from the commensurate positions by $\tau = (0.006, 0, -0.017)$, whereas we found peaks at $\tau = (0.0125, 0, 0.0125)$. The reason for this difference is not clear, although the reduced lattice parameters of our sample, indicative of a possible oxygen deficiency, may be important.

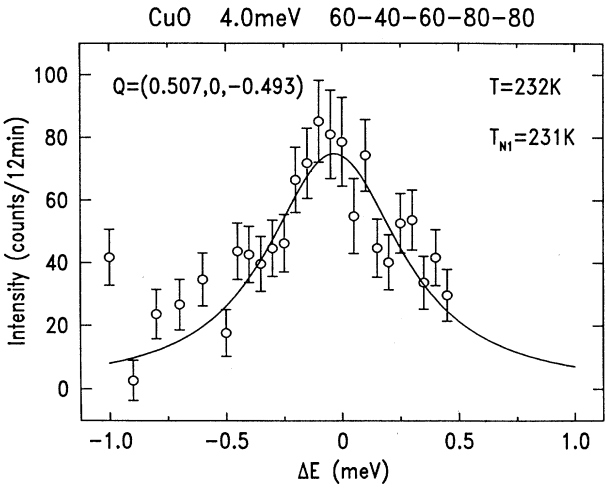

FIG. 9. $T = 231$ K energy scan at $(\frac{1}{2}0\frac{1}{2})$ with the incoherent scattering removed. The half width at half maximum of a similar scan at 250 K would be approximately 2 meV. The line is fit to a Lorentzian convoluted with a one-dimensional Gaussian resolution function.

In another recent paper, Kondo, Ono, Sugiura, and Sugiyama[23] have emphasized the one-dimensional nature of the exchange interactions in CuO. Analyzing the magnetic susceptibility above T_{N1} in terms of the behavior expected for a one-dimensional antiferromagnetic Heisenberg chain,[24] they obtain a J of 69 meV, in excellent agreement with the value estimated from our spin-wave measurements. Quasi-one-dimensional interactions would also be consistent with our observation of magnetic excitations and correlations above T_{N1}. The critical scattering near T_{N1} could be due to interchain correlations. However the degree of anisotropy of the interactions has not been directly determined. Measurements of spin-wave dispersion will be required to resolve this situation.

The most significant result of this work is the observation of a large spin-wave velocity. It suggests that a strong superexchange interaction is intrinsic to linear Cu−O−Cu bonding. Thus, if the strength of the magnetic coupling is in some way important for superconductivity in the layered cuprates, then Cu and O may be a unique combination of elements which are required for high-temperature superconductivity.

ACKNOWLEDGMENTS

We are grateful to R. J. Birgeneau, W. Hardy, and A. Millis for helpful discussions. B. X. Y. and T. R. T. were guest scientists at Brookhaven National Laboratory during the course of this work. The work at Brookhaven was supported by the Division of Materials Science, U.S. Department of Energy, under Contract No. DE-AC02-76CH00016. Research at the University of British Columbia was supported by a grant from the National Science Education and Research Council of Canada. The work at MIT was supported by the National Science Foundation under Contracts No. DMR85-01856 and No. DRM84-18718.

[1]M. Steiner, J. Villain, and C. G. Windsor, Adv. Phys. **25**, 87 (1976).
[2]D. Vaknin, S. K. Sinha, D. E. Moncton, D. C. Johnston, J. Newsam, C. R. Safinya, and H. King, Phys. Rev. Lett. **58**, 2802 (1987).
[3]B. Yang, S. Mitsuda, G. Shirane, Y. Yamaguchi, H. Yamauchi, and Y. Syono, J. Phys. Soc. Jpn. **56**, 2283 (1987).
[4]S. Mitsuda, G. Shirane, S. K. Sinha, D. C. Johnston, M. S. Alvarez, D. Vaknin, and D. E. Moncton, Phys. Rev. B **36**, 822 (1987).
[5]J. M. Tranquada, D. E. Cox, W. Kunnmann, H. Moudden, G. Shirane, M. Suenaga, P. Zolliker, D. Vaknin, S. K. Sinha, M. S. Alarez, A. J. Jacobson, and D. C. Johnston, Phys. Rev. Lett. **60**, 156 (1988); J. Rossat-Mignod, P. Burlet, M. J. Jurgens, J. Y. Henry, and C. Vettier, Physica C **152**, 19 (1988).
[6]G. Shirane, Y. Endoh, R. J. Birgeneau, M. A. Kastner, Y. Hidaka, M. Oda, M. Suzuki, and T. Murakami, Phys. Rev. Lett. **59**, 1613 (1987).
[7]R. W. Millar, J. Am. Chem. Soc. **75**, 2471 (1953).
[8]J.-H. Hu and H. L. Johnston, J. Am. Chem. Soc. **75**, 2471 (1953).
[9]B. N. Brockhouse, Phys. Rev. **94**, 781 (1954) [abstract for APS Annual Meeting (New York)].
[10]M. O'Keefe and F. S. Stone, J. Phys. Chem. Solids **23**, 261 (1962).
[11]B. Roden, E. Braun, and A. Freimuth, Solid State Commun. **64**, 1051 (1987).
[12]G. T. Tunell, E. Posnjak, and C. J. Ksanda, Z. Kristallogr. **90A**, 120 (1935).
[13]H. E. Swanson, E. Tatge, and R. K. Fuyat, *Standard X-ray Diffraction Powder Patterns,* Natl. Bur. Stand. (U.S.) Circ. No. 539 (U.S. GPO, Washington, DC, 1953), p. 1.
[14]S. Åsbrink and L.-J. Norrby, Acta Crystallogr. B **26**, 8 (1970).
[15]B. X. Yang, J. M. Tranquada, and G. Shirane, Phys. Rev. B **38**, 174 (1988).
[16]J. Akimitsu and Y. Ito, J. Phys. Soc. Jpn. **40**, 1621 (1976).
[17]R. J. Birgeneau, H. J. Guggenheim, and G. Shirane, Phys. Rev. B **1**, 2211 (1970).
[18]R. A. Cowley, G. Shirane, R. J. Birgeneau, and H. J. Guggenheim, Phys. Rev. B **15**, 4292 (1977).
[19]W. Marshall and S. W. Lovesy, *Theory of Thermal Neutron Scattering* (Claredon, Oxford, 1971).
[20]T. Thio *et al.*, Phys. Rev. B **38**, 905 (1988); K. B. Lyons, P. A. Fleury, J. P. Remeika, A. S. Cooper, and T. J. Negran, *ibid.* **37**, 2353 (1987).
[21]L. J. DeJongh and A. R. Miedema, Adv. Phys. **23**, 1 (1974).
[22]J. B. Forsyth, P. J. Brown, and B. M. Wanklin, J. Phys. C **21**, 2917 (1988).
[23]O. Kondo, M. Ono, E. Sugiura, and K. Sugiyama, J. Phys. Soc. Jpn. Lett. (to be published).
[24]J. C. Bonner and M. E. Fisher, Phys. Rev. **135**, A640 (1964).